Molecular Characterization of the Receptor−Ligand Complex for Parathyroid Hormone†

Christian Rölz,‡,§ Maria Pellegrini,‡ and Dale F. Mierke*,‡,||

Department of Molecular Pharmacology, Physiology, & Biotechnology, Division of Biology and Medicine, Box G-B4, and Department of Chemistry, Brown University, Providence, Rhode Island 02912

Received December 14, 1998; Revised Manuscript Received March 24, 1999

ABSTRACT: Molecular models for the interaction of parathyroid hormone (PTH) with its G-protein-coupled receptors (PTH1 and PTH2) have been developed. The proposed ligand−receptor complex is based on experimental data from spectroscopic investigations of the hormone and receptor fragments as well as theoretical structure predictions based on homology analysis with proteins of known structure. From the insight afforded by the models, biochemical and pharmacological observations can be correlated with specific molecular or atomic interactions. The ligand selectivity of PTH2, specifically the lack of binding of His^5-containing analogues, can be ascribed to unfavorable steric interactions (the binding pocket is markedly smaller in PTH2 than PTH1) as well as repulsive Coulombic forces between amino acids of like-charge (a positively charged H384 is located in the binding pocket in PTH2). The model of PTH1 suggests that the constitutive activity observed from the incorporation of a positively charged amino acid at position 223, found at the cytoplasmic end of TM2, is caused by a Coulombic attraction to E465, at the cytoplasmic end of TM7, leading to an association of TM2 and TM7 and thereby ligand-free activation. Additionally, a number of important interactions in the ligand−receptor complex are described along with predictions of the pharmacological profile which will result from specific modifications at these sites. In this regard, the models described here allow for atomic insight into the biochemical data currently available and allow targeting of future mutations to probe specific ligand/receptor interactions and thereby further our understanding of the functioning of this important hormone system.

Parathyroid hormone (PTH)[1] plays a major role in the regulation of calcium and phosphate homeostasis. PTH is one of the few bone-active agents proven to be anabolic (*1*) and therefore has been the subject of intensive study (*2*−*4*). The hormone mediates its effects via a G-protein coupled receptor (PTH1) localized in bone and kidney (*5*−*9*).

Parathyroid hormone related protein (PTHrP), evolutionary related to PTH, displays similar binding and pharmacological profiles at PTH1 (*10*). Truncation studies on the native hormones, have shown that the N-terminal peptides, PTH-(1−34) and PTHrP-(1−34), are sufficient for high-affinity binding to and activation of PTH1 (*9*, *11*−*13*). The 15−34 region of these sequences, sharing only minimal sequence homology, see Table 1, contains the principal determinants of binding to PTH1 and can inhibit the binding of either natural ligand, suggesting a common location for interaction on the receptor surface (*13*−*15*). The amino-terminal portion of each hormone, which is highly conserved with 8 out of 13 residues being identical (Table 1), is essential for activation of PTH1. On the basis of the similar pharmacological profiles of PTH-(1−34) and PTHrP-(1−34), it seems likely that both ligands will interact with PTH1 in a similar fashion.

In 1995, a second receptor for parathyroid hormone (PTH2) was discovered (*16*). Although sequentially related to PTH1 (51% amino acid sequence identity), the ligand selectivity was markedly different: while PTH1 responds fully to both PTH and PTHrP, PTH2 responds only to PTH (*16*−*18*). From mutation studies, residue 5 was found to be an important switch in the ligand selectivity observed for PTH2 (i.e., Ile^5 containing PTHrP activated PTH2) (*17*, *19*) Furthermore, the Ile^5-PTHrP analogue competed against PTH binding. These results suggest that the ligand selectivity of PTH2 is localized around the binding site for residue 5. To understand the underlying mechanism responsible for this ligand selectivity, we undertook the generation of molecular models of the ligand−receptor complexes for both PTH1 and PTH2.

The molecular models were assembled using structural building blocks obtained by NMR spectroscopy and by computer modeling using structurally related proteins as templates (rhodopsin) and sequentially homologous proteins

† This work was supported, in part, by Grant R29-GM54082 from the National Institutes of Health (D.F.M.) and Grant 98/02903 from the Deutscher Akademischer Austauschdienst (C.R.).

* To whom correspondence should be addressed. Phone: (401) 863-2139. Fax: (401) 863-1595. E-mail: Dale_Mierke@Brown.edu.

‡ Department of Molecular Pharmacology, Physiology, & Biotechnology.

§ Permanent address: Department of Organic Chemistry and Biochemistry, Technical University of Munich, Lichtenbergstr. 4, D-85747 Garching, Germany.

|| Department of Chemistry.

[1] Abbreviations: Bpa, benzoyl phenylalanine; DG, distance geometry; DPC, dodecylphosphocholine; EC, extracellular loop; G-Protein, guanine nucleotide-binding regulatory protein; GPCR, G-protein coupled receptor; MD, molecular dynamics; NOE, nuclear Overhauser enhancements; NOESY, nuclear Overhauser enhancement spectroscopy; PTH, human parathyroid hormone; PTHrP, parathyroid hormone-related protein; PTH1, parathyroid hormone receptor 1; PTH2, parathyroid hormone receptor 2; PDB, Brookhaven protein data bank; TM, transmembrane.

10.1021/bi9829276 CCC: $18.00
Published on Web 04/30/1999

Table 1: Sequence Alignment of Human Parathyroid Hormone PTH-(1−34) and Human Parathyroid Hormone Related Peptide PTHrP-(1−34)[a]

Protein	Sequence Alignment			
	1	10	20	30
PTH	SVSEIQLMH	NLGKHLNSME	RVEWLRKKLQ	DVHNF
conserved[b]	+VSE QL+H	+ GK + +	R +L +	++H
PTHrP	AVSEHQLLH	DKGKSIQDLR	RRFFLHHLIA	EIHTA

[a] Sequences are given in amino acid one-letter code. [b] The + symbol denotes similar amino acids as defined by Altschul (*32*).

of known structure. Docking of the hormone to the receptor utilized contact points provided by photoaffinity cross-linking investigations (*20*−*23*). The two contact points Ser[1]-M425 and Lys[13]-R186 between the ligand and receptor,[2] coupled with the high-resolution structure of PTH-(1−34), provided different topological arrangements and orientations of the ligand when associated with the receptor (*22*). These structures were utilized as starting points for extensive molecular dynamics (MD) simulations employing a water/decane/water three-phase box (*24*), that mimics the native membrane environment and still results in reasonable simulation times. The resulting models for the PTH−PTH1 and PTH−PTH2 complexes allow for molecular insight into the numerous biochemical and mutational studies which have been reported for this receptor system. More importantly, the models described here provide a working hypothesis for the formation of the hormone−receptor complex, and the mechanism by which the ligand association leads to receptor activation. As a working hypothesis, our model will require modification and refinement. To further this effort, specific mutations that will probe interactions deemed important in the model are included here along with predictions of the pharmacological consequences.

MATERIALS AND METHODS

The generation of the transmembrane (TM) portion of PTH1 and PTH2 was carried out with the WHATIF program (*25*). The method utilizes rhodopsin and bacteriorhodopsin (*26*−*29*) as templates for the topological orientation and arrangement of the seven TM helices. Addition of the connecting loops and termini to the TM helices completed the receptor model. The loops were produced using a metric-matrix based DG program, using the distances between adjacent TM helices as constraints.

For PTH1, the conformational features of the receptor fragment, PTH1(168−198), in a lipid environment, as determined by NMR (*30*), was incorporated into the model. The receptor fragment displayed a membrane embedded hydrophobic helix (consisting of residues 190−196, corresponding to the beginning of TM1) preceded by two amphipathic helices (consisting of residues 169−176 and 180−189, respectively) which were shown to be located on the surface of the lipid micelle (*30*). Following previously published procedures (*22, 31*), the BLAST program (*32*) was used to search for homologous regions between the loops and termini of the receptors and proteins of known structure within the Brookhaven Protein Data Bank (PDB) (*33*). The homologous region of the protein of known structure was then analyzed for secondary structure. In the cases where multiple occurrences of similar secondary structure were observed for a region of the receptor, the secondary structure was incorporated into the model. Given the difficulty in determining the partner strand in the formation of a β-sheet, this homology analysis was restricted to α-helices.

The resulting receptor was energy minimized and subjected to a short MD run using the DISCOVER program (Biosym Technologies) in order remove initial strains. During this stage, the backbone topology of the TM helices was preserved by constraining all backbone heavy atoms to their initial positions. Similarly, the secondary structure of the loops and termini determined experimentally or predicted from sequence homology was maintained using dihedral angle restraints.

The receptor was then placed in a three-layer (water/decane/water) simulation cell for further refinement by short MD simulations. The TM helices were placed in the decane layer while the extra- and intracellular regions were embedded in the water phases. The membrane environment was mimicked by a layer of approximately 40 Å of decane molecules, with approximately 30 Å layers of water above and below, consisting of approximately 700 decane and 20 000 water molecules (*24*). The solvent system sacrifices the charged nature of the lipid/water interface for computational simplicity while maintaining the overall biphasic, hydrophobic/hydrophilic character as well as the molecular motions of the long acyl chains found in membranes (*24*). All solvated simulations were carried out using the GROMACS package (*34*).

The modeling of the ligand−receptor complex utilized the structure of PTH-(1−34) that was previously determined in a micellar-lipid environment in our laboratory (*35*). The experimentally determined helical domains (3−10 and 21−32) were maintained during all subsequent simulations by application of dihedral angle restraints. The structural features of the ligand in the zwitterionic, lipid environment was important given the proposed membrane-associated pathway for interaction with the receptor. The N- and C-terminal helices in PTH have been observed previously, although these studies usually utilized trifluoroethanol in an effort to stabilize the helices (*36*−*41*).

Starting structures of each receptor−ligand complex were generated by docking PTH-(1−34) to PTH1 or PTH2. The docking strategy applied was essentially identical for both receptors. The N-terminal helix of PTH was placed slightly above its putative binding site at the extracellular surface, above the central core of the TM helical bundle. Backbone dihedral angles of the connecting flexible region, residues 13−19, were rotated manually until the C-terminal helix was on the plane of the membrane interface in proximity to the helical domain PTH1(180−189) of the N-terminus of the receptor. The contact points generated from the photoaffinity cross-linking studies (Ser[1]-M425 and Lys[13]-R186 of the ligand and receptor, respectively) (*21, 22*) were converted into distance constraints of 10 Å and employed in a subsequent simulated annealing run (in vacuo) carried out with the DISCOVER program. On the basis of the sequence homology between PTH1 and PTH2, we assume that the ligand binds to both receptors in a similar manner, and

[2] To simplify the description of the interactions in the ligand−receptor complex, the amino acids of the ligand will be denoted using the three-letter code, while the one letter code will be used for the residues of the receptor.

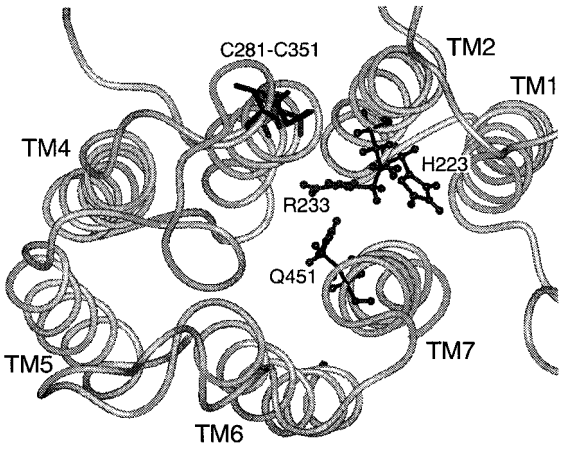

FIGURE 1: Illustration of some key residue−residue contacts within the seven transmembrane helix bundle of PTH1. These contacts (see text) support that the model contains the correct topology of the 7 TM helices.

therefore the contact points involving PTH1 residues were transferred to the homologous residues in PTH2.

The resulting ligand−receptor complexes of low energy were then soaked in a three-layer (water/decane/water) simulation cell as described above. The refinement consisted of three stages. In the first stage, only the solvent was energy minimized and equilibrated in a subsequent 50 ps MD run at 300 K, while the hormone−receptor complex was frozen in its initial conformation. The constraints were then released and the whole system energy minimized. In stage two, 200 ps restrained MD at 300 K was performed with the same distance restraints between hormone and receptor as applied during the docking. Finally, the distance restraints were removed and the system allowed to freely evolve during another 200 ps of MD at 300 K. All simulations were carried out using periodic boundary conditions. Neighbor lists were updated every 10 steps. Only nonbonded interactions within 8 Å (Lennard-Jones) and 10 Å (Coulomb) were included. Temperature bath coupling with a time constant of 0.02 ps was applied (*42*). All calculations were performed on an SGI Origin 2000 computer.

RESULTS AND DISCUSSION

Modeling of the PTH1 Receptor. The general applicability of the structural features of the TM helices of rhodopsin and bacteriorhodopsin as templates has been addressed in some detail in the literature (*43*−*46*). To probe the use of the template for PTH1, the TM domain model was checked for consistency with published mutational data. According to Gardella et al., mutations of R233 (TM2) and Q451 (TM7) affect signaling and binding of PTH-(1−34) (*47*). Results from the double mutant receptor, in which both R233 and Q451 are modified, provide evidence of an interaction between these two sites (*47*). In our model, both residues are located in the middle of their respective TM helices projecting toward each other as illustrated in Figure 1. It is important to stress that this mutational data was not used in the generation of the model.

Recently, it has been reported that the mutations H223R and H223K lead to constitutively active receptors leading to Jansen's metaphyseal chondrodysplasia (*48, 49*). In the receptor model, this residue is located at the intracellular end of TM2 projecting toward TM7 (see Figure 1). It is believed that the activation of GPCRs involves the interaction between TM2 and TM6 or TM7 (*46*), and therefore, the orientation of H233 toward TM7 can be taken as support for the correct topology of the seven TMs in the model. In addition, considering that only positively charged residues at position 223 induce constitutive activity, it seems likely that a Coulombic attraction to a negatively charged residue (on TM6 or TM7) could account for this effect. In our model, one obvious candidate is E465, on the cytoplasmic end of TM7. We propose that this favorable charge−charge interaction leads to the constitutively active PTH1 by maintaining an arrangement in which TM2 and TM7 are in close proximity.

The mutation T410P has also been shown to lead to constitutive activity associated with Jansen's disease (*48*). In our model this residue is located in the upper half of TM6. Introduction of a helix-breaking proline in addition to the naturally occurring P415 leads to a severely distorted helix geometry which we postulate accounts for the observed constitutive activation. Recently, a preliminary report describing an additional mutation, I458R, which leads to constitutive activity appeared (*50*). This amino acid, similarly to amino acid 451 described above, projects into the helical bundle. Replacement with a positively charged residue could significantly alter the interaction with other TM helices. A more in-depth investigation of these mutant receptors will be carried out in the future.

Two different sources were employed for obtaining structurally relevant data used as starting points in the generation of the extracellular regions of PTH1: experiment-based spectroscopic studies and theoretical-based homology analysis. The NMR-derived structure of the receptor fragment, PTH1(168−198), consisting of the N-terminus proximal to TM1, was incorporated into the model. Homology modeling, following published procedures (*22, 31*), was used in an attempt to obtain structural information for the extracellular loops. The homologous structures identified for extracellular loops 1 (EC1) and 2 (EC2) were not sufficient to reliably predict the secondary structure (i.e., no regions with multiple hits of similar structure were observed). Therefore, the conformational features of EC1 and EC2 are restricted solely by a disulfide linkage between C281 and C351 in EC1 and EC2, respectively (*51*). Although this bond does not confer a great deal of conformational stability to EC1 which is more than 30 residues in length, the conformational space accessible to EC2 (consisting of approximately 15 residues) is considerably reduced. The homology search for EC3 resulted in a number of homologous regions as reported in Table 2. A comparison of the corresponding secondary structure motifs suggests that EC3 adopts a helical conformation, particularly in the central portion consisting of T435-Y443. During the subsequent MD simulations in a membrane mimicking environment, the helix in EC3 is found to lie at the water/decane interface with its hydrophobic face (L436, V439, and M441) projecting toward the decane phase. As a result, W437 and Q440 are directed toward the center of the TM bundle. As elaborated below, these latter two residues form a hydrophobic pocket for Val^2 of the ligand, in agreement with mutational studies (*51*).

Modeling of the PTH-2 Receptor. The modeling strategy for PTH2 was identical to that outlined for PTH1, justified

Table 2: Sequences and Secondary Structure Motifs[a] of PDB Structures Homologous to the Third Extracellular Loop (425−448) of the PTH-1 Receptor[b]

Protein[c]	Region	Sequence Alignment	Motif
PTH1R	424-447	FMATPYTEVSG**TLWQVQMHY**EMLF	helix
1csy	83-91	**TLWQLVEHY**	helix
1eri	238-256	YTQGDGREW**DSKIMFEIMF**	helix
1nar	173-178	**HYQKLY**	helix
1frt	134-146	PETD**IVGNLWMKQ**	helix
1aqj	380-388	**MQKHVRTLY**	helix

[a] The secondary structure refers to the residues printed in bold. [b] Sequences are given in amino acid one-letter code. Proteins are identified by their PDB entry names. [c] PDB entry names correspond to the following proteins: 1csy, Syk tyrosine kinase C-terminal Sh2 domain complexed with a phosphopeptide from the γ chain of the high affinity immunoglobin G receptor, NMR; 1eri, Eco Ri Endonuclease (Endodeoxyribonuclease Ecori) (E.C. 3.1.21.4) complexed with DNA (Tcgcgaattcgcg); 1nar, Narbonin; 1frt, Fc Receptor (Neonatal) complexed with Fc (Igg) (Fcfcrn complex); 1aqj, adenine-N6-DNA-methyltransferase taqi.

Table 3: Sequences and Secondary Structure Motifs[a] of PDB Structures Homologous to the N-terminal Peptide 121−151 of the PTH-2 Receptor[b]

Protein[c]	Region	Sequence Alignment	Motif
PTH2R	121-151	NYSDCLRF**LQPDISIGKQE**FFERLYVMYTVG	helix
1aj3	73-88	**LSDD**NTIG**KEEIQQRL**	helix
1lhs	17-36	V**EPDLSAHGQEVIIRLFQL**H	helix
3ldh	131-146	DCLKELHPEL**GTDKNK**	helix
7r1r	366-382	**DAFFA**D**QEEFERLYTKY**	helix

[a] The secondary structure refers to residues printed in bold. [b] Sequences are given in amino acid one-letter code. Proteins are identified by their PDB entry names. [c] PDB entry names correspond to the following proteins: 1aj3, solution structure of the spectrin repeat, NMR; 1lhs, Loggerhead Sea Turtle myoglobin (Aquo-Met); 3ldh, lactate dehydrogenase (E.C. 1.1.1.27) M4 enzyme, ternary complex with nad and pyruvate; 7r1r, ribonucleotide reductase E441q mutant R1 protein from *Escherichia coli*.

by the high homology of the two receptors, particularly with respect to the transmembrane domains. As no experimental structure was available for the N-terminus, it was also included in the search for sequentially homologous structures in the PDB. A number of hits was obtained for the long N-terminus suggesting different helical regions. However, since the tertiary packing of the putative helices is unknown, this information was not further utilized in the modeling efforts with the exception of the helix closest to TM1, starting at L129 (L129-E139). This helix closely resembles the helix experimentally verified for PTH1 (*30*); the helix is amphipathic and thus likely to reside at the membrane/water interface, similarly to what was experimentally verified for the corresponding helix in PTH1. The sequences obtained from the PDB for this helix are listed in Table 3. No secondary structural elements could be ascertained for the extracellular loops of PTH2.

Docking of PTH-(1−34) to PTH1 and PTH2. The cross-linking and receptor mutational results, coupled with the known structure of the ligand, provide sufficient data for defining the binding mode between the N-terminus of the ligand and receptor. In contrast, with the exception of one cross-linking point, there is no data available for the C-terminal helix of PTH. The cross-linking point between residues 33 and 37 of PTH1 with position 23 of a PTHrP analogue (*23*), although providing evidence that the N-terminus plays a role in ligand binding, cannot be translated

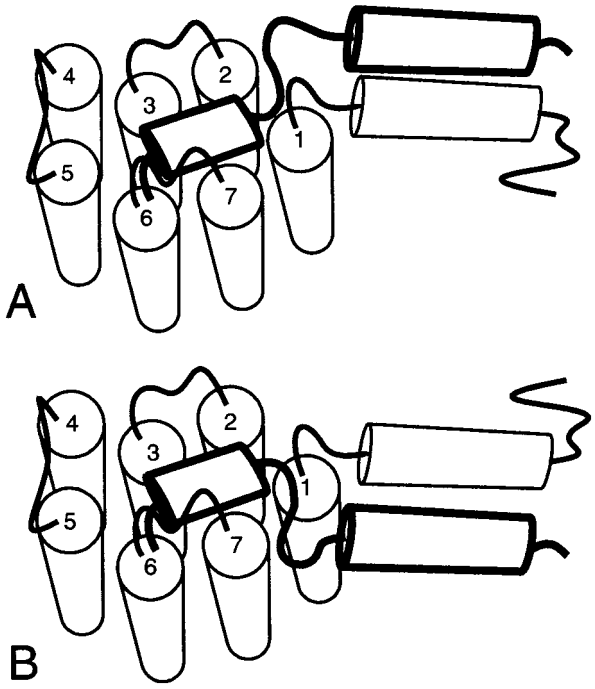

FIGURE 2: Schematic representation of alternative binding modes for the C-terminal helix of PTH (thick lines) with the N-terminus of the receptor. Experimental data indicate that the helix of the ligand, as well as the receptor fragment proximal to TM1 (residues 168−180), are membrane associated.

into structural insight: the unknown structural features of the long N-terminus of the receptor (particularly the domain between residues 37 and 168), allow for too many different structural arrangements to be explored by computational approaches alone. However, a closer inspection of the NMR-derived structures of PTH and the fragment of PTH1, PTH1-(168−198), containing the residues cross-linking to Lys^{13} of PTH, suggests a possible mode of interaction (*30, 35*). The NMR studies of PTH in the presence of DPC micelles indicate that the C-terminal helix of the ligand is membrane associated, through a hydrophobic face, consisting of Val^{21}, Leu^{24}, Leu^{28}, and Val^{31}. This binding domain of the ligand is thought to interact in an antiparallel arrangement with the N-terminus of the receptor, specifically the helix-spanning residues 180−189 (*22*). As illustrated in Figure 2, two possible orientations of the domains can be envisioned. This region in PTH1 and PTH2 contains a large number of charged amino acids (**PTH1**, E177, R179, E180, R181, E182, D185, R186; **PTH2**, R127, D132, K137, E139). Taken together with the charged nature of the C-terminal helix of the ligand (Glu^{22}, Arg^{25}, Lys^{26}, Lys^{27}, Asp^{30}), it seems likely that Coulombic interactions play a decisive role in the recognition process. Both of the interaction modes depicted in Figure 2 were built for PTH1 and PTH2, and extensive MD simulations carried out.

Interactions between Ligand and Receptor. Unfortunately, the calculations did not show a clear energetic distinction between the two binding motifs illustrated in Figure 2. The interactions between the C-terminal helix of PTH and the receptor were equally favorable, including different combinations of the Coulombic interactions listed above. It is clear that the definition of this binding mode between receptor and ligand will have to await additional experimental data. On the other hand, the current model provides great insight

into the interactions between the N-terminal portion of the ligand (activation domain) and the receptor. These interactions are described in detail below.

Binding Site of PTH Residue Ser[1]. In both PTH1 and PTH2, the N-terminal residue of PTH is located on or near the top of TM6 and EC3. In the case of PTH1, the positively charged amine of Ser[1] is hydrogen bonded to the backbone carbonyl groups in the last turn of TM6 (involving residues A426, T427, and P428) stabilizing the macrodipole of the helix (positive charges are often observed at the C-terminal ends of α-helices in protein structures). In PTH2, Ser[1] is slightly rotated to produce a hydrogen bond between its carbonyl and the amide proton of F386 but is still in spatial proximity to the extracellular end of TM6 (H384, S385, and F386). Replacement of Ser[1] by Ala[1] as found in PTHrP should have only minor effects on the binding affinity as both residues are of similar size and no specific interactions of the hydroxyl function of serine were identified.

In the model of PTH1, M425 is located on the extracellular end of TM6 projecting into the membrane, away from the core of the TM-helix bundle and away from Ser[1] of PTH (*22*). The discrepancy between results of the simulations and cross-linking studies (indeed, Ser[1] cross-links to M425) can be attributed to the difference in size and hydrophobic nature of the side chains of serine and benzoyl phenylalanine (Bpa), utilized for the cross-linking experiments. While the small, polar serine fits nicely into the pocket produced by TM6 and EC3, the bulky hydrophobic benzophenone moiety of Bpa cannot be accommodated and instead seeks the hydrophobic environment of the membrane, projecting out between TM5 and TM6. This orientation places the photoreactive moiety in close proximity to M425 accounting for the cross-linking data. This is a clear indication that the modification of the ligand required for the photoaffinity cross-linking studies (e.g., incorporation of Bpa) must be carefully considered in the development of detailed molecular models. The photoactive species of Bpa is reported to have a range of 3.1 Å for cross-linking (*52*). In the modeling efforts described here, we have utilized distance restraints of 10 Å between the cross-linked residues to allow for variability and flexibility in finding low-energy binding modes and to account for the modifications of the natural amino acids of the ligand.

Binding Pocket of PTH Residue Val[2]. Both PTH1 and PTH2 accommodate Val[2] in a hydrophobic pocket formed by EC3 (**PTH1**, L436, W437, Q440; **PTH2**, T387, W391). The binding pocket is a direct result of the lack of conformational freedom of EC3, either by the presence of an α-helix (PTH1) or small size (only 13 residues for PTH2). These hydrophobic pockets are complemented by residues in the C-terminal end of EC2 (**PTH1**, K359, K360, I362; **PTH2**, I317, Y318). Many of these interactions are depicted in Figures 3 and 4.

According to Lee et al. (*51*), substitution of W437 (with A, L, or E) or Q440 (with A or L) in PTH1 leads to a loss in binding affinity for PTH-(1−34), an effect much reduced with PTH-(3−34). Our model provides molecular insight into these mutations. W437 and Q440 are located on the same face of the EC3 helix, projecting toward the center of the TM bundle. Their side chains participate in the hydrophobic pocket for Val[2], shielding this residue from the aqueous environment on the extracellular surface of the membrane.

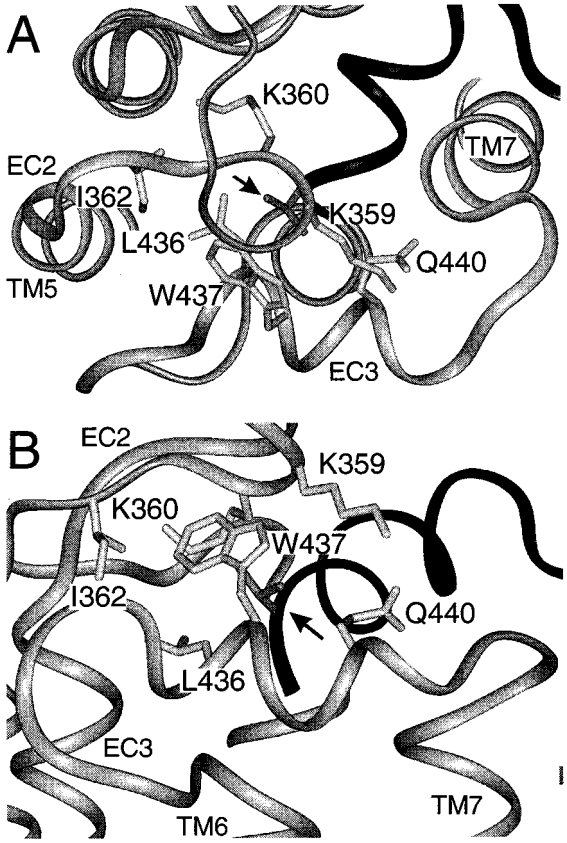

FIGURE 3: Illustration of the binding pocket for valine-2 of PTH in PTH1 (panel A, top view, panel B, side view). The receptor and ligand are depicted as ribbons in gray and black, respectively. The black arrow indicates valine-2.

Thus, mutating W437 and/or Q440 to any smaller or more polar amino acid would disrupt the binding pocket exposing Val[2] to water or lead to unfavorable interactions with this residue. However, in absence of Val[2] the effect would be much less pronounced, as was indeed observed for PTH-(3−34). Our model also accounts for the observed increase, albeit small, in binding affinity of PTH-(1−34) in the case of the Q440R mutation. From our model, placement of a positively charged arginine at position 440 would lead to a favorable Coulombic interaction with Glu[4] of PTH, while maintaining the hydrophobic pocket for Val[2] of the ligand. Recently, similar mutations have been carried out in conjunction with swapping or deletion of the e2 segment of the N-terminus (*53*). These data indicate a role for the EC3 loop in receptor binding and receptor selectivity, affected by the distal e2 region of the N-terminus.

Binding Pocket of PTH Residue Ile[5]. Considering the importance of residue 5 of PTH/PTHrP for ligand selectivity (*17, 19*), one might expect pronounced differences in the topology of the binding sites for this residue. This is indeed the case. In PTH1, the Ile[5] side chain is accommodated in a hydrophobic pocket made up of the extracellular ends of TM3 (A284, and V285) and TM7 (F447) which form the bottom of the pocket, as illustrated in Figures 5 and 6. The binding cavity extends deep into TM3, TM4, TM5, and TM6 (Figure 7, panels A and B); there is sufficient space to accommodate either isoleucine or histidine residues. It is important to point out that the experimental cross-linking data utilized here is for PTH. It is not clear that PTH and PTHrP bind to the receptor in identical manners (*54*). Results

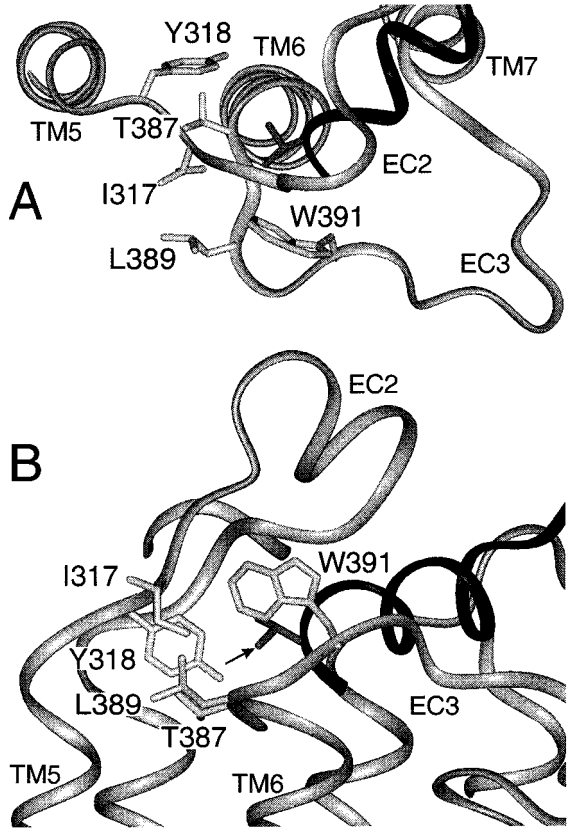

FIGURE 4: Illustration of the binding pocket for valine-2 of PTH in PTH2 (panel A, top view, panel B, side view). The receptor and ligand are depicted as ribbons in gray and black, respectively. The black arrow indicates valine-2.

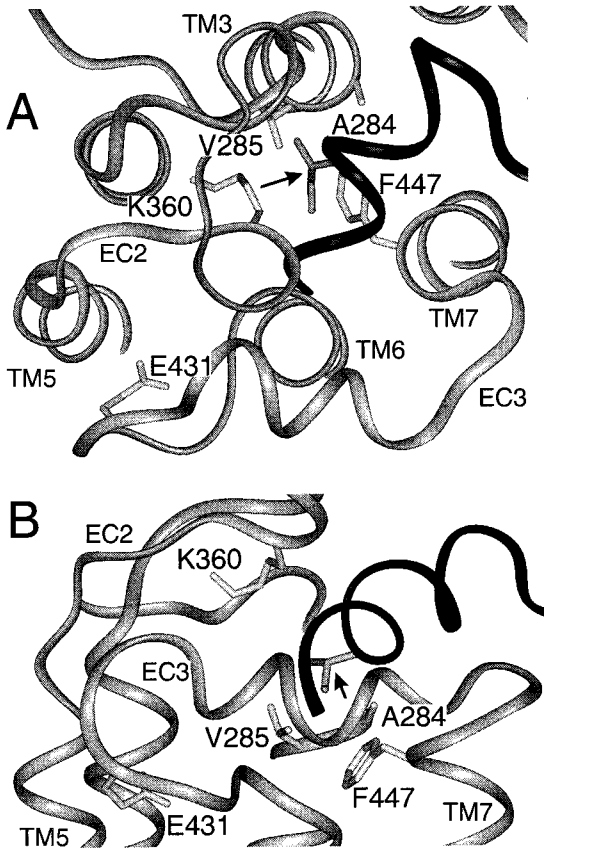

FIGURE 5: Illustration of the binding pocket for isoleucine-5 of PTH in PTH1 (panel A, top view, panel B, side view). The receptor and ligand are depicted as ribbons in gray and black, respectively. The black arrow indicates isoleucine-5.

from PTH/PTHrP chimera (*55*) coupled with structural characterization of the hormones (*35*, *54*) would indicate that the two hormones bind differently, particularly evident in the C-terminal binding domain, where a shifting of the C-terminus has been proposed (*54*). This shifting in the C-terminal domain could lead to altered orientations of the N-terminus within the seven helical TM bundle. In the current analysis, we assume the N-termini of PTH and PTHrP interact with the receptor similarly.

The binding pocket for residue 5 in PTH2 involves the corresponding regions as noted for PTH1. This is in agreement with recent results from Bergwitz et al. that show via cassette and point-mutations that the extracellular ends of TM3 and TM5 play a role in the binding of Ile^5-containing ligands to PTH2 (*56*). One major difference in the binding pocket for PTH2 is the size, limited by F386 and F401 on the extracellular ends of TM6 and TM7, respectively. With the smaller size, the binding pocket can no longer accommodate His^5. Besides this steric contribution, Coulombic interactions may also play a role in the poor binding of His^5-containing ligands. A sequence alignment of the TM6/EC3 region for the two receptors, as shown in Table 4, reveals an insertion of a glutamate (E431) in PTH1 with respect to PTH2. Although in our model this residue is not part of the binding pocket, its presence at the entrance of the cavity could assist in the binding of PTHrP by attracting the positively charged His^5. This is a unique feature of PTH1, with no equivalent in PTH2. Instead, in PTH2 at the bottom of the binding pocket for residue 5, there is a positively charged H384 (Table 4) that further destabilizes the PTHrP−PTH2 complex, accounting for the poor affinity of His^5-containing analogues to PTH2 (Figure 7C).

Recently, Turner et al. replaced the N-terminus and positions 397 and 400 of PTH2 with the corresponding residues from PTH1, producing a mutant receptor which is activated by PTHrP (*57*). The two point mutations in this receptor (C397Y and F400L) are found on the extracellular end of TM7. Although F400 is in close proximity to the binding site of residue 5, it is directed toward TM6 and therefore does not directly interact with residue 5. One could hypothesize indirect effects caused by these mutations, effects that modify the binding pocket of position five of the hormone, allowing for compatibility with a His^5-containing ligand. Indeed, the adjacent residue F401 forms the bottom of the Ile^5-binding pocket in PTH2. Due to a lack of experimental information on the secondary structure of EC3 of PTH2 at this stage, no rationale can be given for the observed behavior of the C397Y mutant. It is important to keep in mind that in the interpretation of receptor mutational data we are using a static representation of the ligand−receptor complex while the activation of the receptor, as well as desensitization, internalization, and resensitization, are all dynamic events. Given the dynamic life-cycle of the receptor, it is not surprising that a few mutations, particularly those associated with activation of the receptor, cannot be described by the interpretation of static binding interactions.

Binding Pocket of PTH Residue Met^8. Continuing along the N-terminal α-helix of the ligand, the next amino acid along the same helical face of Ile^5 is Met^8. In both PTH1

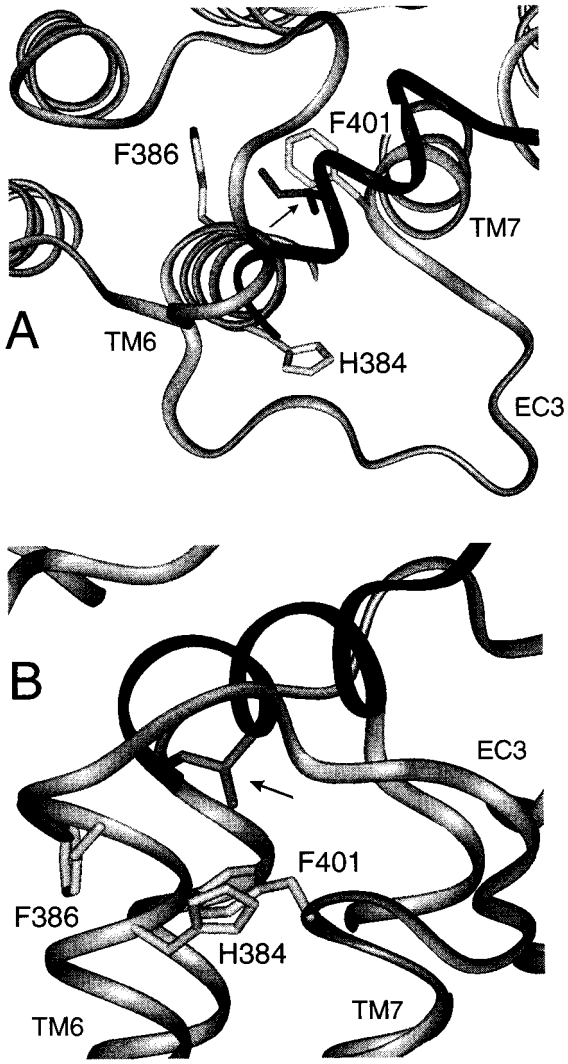

FIGURE 6: Illustration of the binding pocket for isoleucine-5 of PTH in PTH2 (panel A, top view, panel B, side view). The receptor and ligand are depicted as ribbons in gray and black, respectively. The black arrow indicates isoleucine-5.

and PTH2 complexes, the Met[8] is found in deep hydrophobic clefts (**PTH1**, K240, A284, F447; **PTH2**, R143, L144, F400, F401, N402) made up of the extracellular termini of TM1, TM2, and TM7. These hydrophobic pockets are in agreement with the observation that oxidation of Met[8] results in a decrease in the biological response (*58*). The replacement of Met (both 8 and 18) in PTH with nor-leucine is well tolerated, producing no loss of binding affinity (*59*). The preceding residue, the hydrophobic Leu[7], is observed to favorably interact with these same hydrophobic pockets of the receptor.

Given the helical structure of the N-terminus, the remaining amino acid residues project away from the seven TM helical bundle, interacting with the extracellular loops which are partially folded over the ligand or remain solvent exposed. The specific ligand/receptor interactions will be much better defined after the structural features of the EC loops have been experimentally determined, efforts which are currently ongoing. The role of these other residues could be to maintain or stabilize the N-terminal α-helix. Noting that residues 3 and 6 are highly conserved in PTH and PTHrP, Nissenson and co-workers examined these two sites both for helix stability and receptor binding and activation (*60*). The study

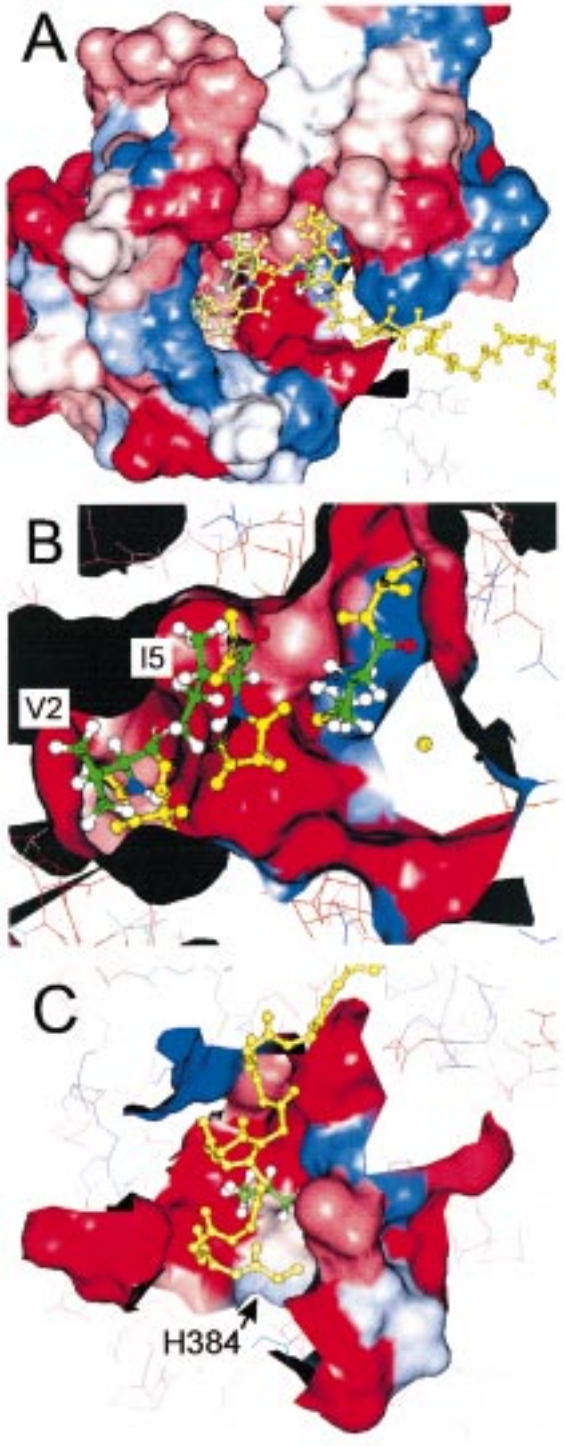

FIGURE 7: The binding pocket for the N-terminus of PTH in PTH1 (panels A and B) and PTH2 (panel C). The receptor surface is colored according to a hydrophobicity scale (red = hydrophobic, blue = charged). The ligand is depicted in ball-and-stick in yellow, with the exception of residues, valine-2, isoleucine-5, and methionine-8, colored by atom-type. Panel A illustrates the folding of the extracellular loops over the ligand. In panel B, the extracellular loops have been cut away to show the hydrophobic pocket for valine-2 and isoleucine-5. The binding pocket for isoleucine-5 in PTH2 is shown in panel C. The positioning of H384 within this binding pocket, which accounts for the lack of affinity of histidine-5 containing ligands, is highlighted.

showed that large, bulky residues were not well tolerated at position 3, which the authors hypothesized could inhibit interaction with the receptor (*60*). We propose that the mostly

Table 4: Sequence Alignment of the Region around the Extracellular End of TM6[a]

Receptor	Region	Sequence Alignment[b]
PTH1R	424-435	FMATPYT**E**VSGT
PTH2R	379-389	FVCLP**H**S.FTGL

[a] Charged residues are printed in bold face. [b] Sequences are given in amino acid one-letter code. The alignment was performed by the Gap program of the GCG software package (Madison, WI). The dot denotes a gap in the PTH2R sequence.

hydrophobic amino acids examined would lead to a rotation of the N-terminal helix of the ligand, in an attempt to bury this position, disrupting many of the interactions described above. A similar mechanism can explain the observation reported for the replacement of Gln^6 (*60*). Only the incorporation of Glu at this position would maintain the similar placement of the N-terminal helix of the ligand and therefore be expected to maintain the biological activity of PTH.

In addition to providing insight into mutational data already in hand, the molecular models can be used to identify amino acids with important roles in ligand binding. The modification of these residues, coupled with the pharmacological characterization of the mutant receptor, would assist in the further refinement of the model. As detailed above, the ligand selectivity displayed by PTH2 arises from a combination of steric as well as Coulombic interactions at position 5 of the hormone. While PTH1 offers a large hydrophobic pocket that can readily accommodate both Ile and His, the available space in the corresponding binding site of PTH2 is limited by bulky aromatic side chains (F386 and F401) on the extracellular end of TM6 and TM7. Replacing these residues by smaller, hydrophobic ones (L, V, A) could enlarge the cavity and thus enable PTH2 to bind His^5 without steric hindrance. The introduction of bulky hydrophobic residues in the corresponding positions of PTH1 (A426 and T427 in TM6) could in turn diminish the size of the binding pocket and introduce ligand selectivity to PTH1. To probe the role of charged residues unique to either PTH1 (E431) or PTH2 (H384) in ligand selectivity, these residues could be substituted by polar but uncharged amino acids of similar size (e.g., E431Q and H384Q). The E431Q PTH1 receptor is predicted to display reduced PTHrP affinity, while H384Q PTH2 will restore PTHrP affinity.

During the simulations of the ligand−receptor complexes, the extracellular loops fold over the central core of the TM bundle and the ligand-binding pocket. We have attributed this movement, mainly of EC2 and EC3, resulting in the burying of the first four residues of the ligand, to a high-affinity binding state (Figure 7A). Before the loops make this conformational adjustment, it should be relatively easy for the ligand to dissociate from the receptor. For many other GPCRs clearly measurable, high and low affinity binding has been described (*61*−*64*).

At the current stage, with limited data regarding the structure of the N-terminus of the receptor and its interaction with the C-terminal binding domain of the ligand, we can only hypothesize the mechanistic details of ligand binding. According to the theory introduced by Schwyzer (*65*−*68*), the recognition of peptide hormones by membrane-bound receptors is preceded by nonspecific adsorption on the target cell membrane followed by random lateral diffusion into the binding site. We have employed this theory of initial ligand/receptor interaction and recognition in the development of our two possible binding modes depicted in Figure 2. Indeed, all of the experimental data in hand today, including the studies on the ligands PTH and PTHrP and fragments of the receptor, support a membrane associated pathway. The structural features of the entire N-terminus of the receptor will supply a great deal of insight into the events associated with ligand recognition and binding. Efforts along these lines are currently underway in our laboratory. Such a structure would allow for the utilization of the third cross-linking point (*23*), as well as the results from numerous mutational studies (*47, 53*), in the current molecular model.

CONCLUSIONS

Molecular models for the ligand−receptor complex for the calciotropic hormone, parathyroid hormone, have been presented. The models are based to a large extent on experimental data and refined with computational simulations in which we have attempted to maintain the overall hydrophobic/hydrophilic character of the membrane environment. The insight provided by these models certainly surpasses the serpentine sketches previously employed and may allow for rational design of ligands removed from the natural hormone. The model also allows for the generation of ideas on receptor activation. The interactions of the N-terminal portion of the ligand with EC3 and extracellular ends of TM6 and TM7, while the C-terminal portion of the ligand is engaged with the N-terminus of the receptor, suggests that the role of ligand binding is to bring TM6 and TM7 in juxtaposition to the bundle of the remaining TM helices. Such motions of TM helices would have a direct effect on the conformation of the third intracellular loop, which has been shown to be coupled with both Gs and Gq *(55*). Similar models for receptor activation have been proposed for other GPCRs; the NK1 receptor being the farthest advanced (*69, 70*). This hypothesis certainly requires further testing. The model provides well-targeted modifications that will facilitate these tests. The models presented here are the result of the first iteration, of a process that may require many iterations.

REFERENCES

1. Dempster, D. W., Cosman, F., Parisien, M., Shen, V., and Lindsay, R. (1993) *Endocr. Rev. 14*, 690−709.
2. Potts, J. T., Jr., Kronenberg, H. M., and Rosenblatt, M. (1982) *Adv. Protein Chem. 35*, 323−396.
3. Chorev, M., and Rosenblatt, M. (1996) in *Principles of Bone Biology* (Bilezikian, J. P., Raisz, L. G., and Rodan, G. A., Eds.) pp 305−323, Academic Press, New York.
4. Potts, J. T., Jr, Gardella, T. J., Jüppner, H., and Kronenberg, H. M. (1996) *J. Endocrynol. 154*, S15−S21.
5. Suva, L. J., Winslow, G. A., Wettenhall, R. E., Hammonds, R. G., Moseley, J. M., Diefenbach-Jagger, H., Rodda, C. P., Kemp, B. E., Rodriguez, H., and Chen, E. Y., et al. (1987) *Science 237*, 893−896.
6. Abou-Samra, A. B., Uneno, S., Jueppner, H., Keutmann, H., Potts, J. T., Jr., Segre, G. V., and Nussbaum, S. R. (1989) *Endocrinology 125*, 2215−2217.
7. Iida-Klein, A., Varlotta, V., and Hahn, T. J. (1989) *J. Bone Miner. Res. 4*, 767−774.
8. Jüppner, H., Abou-Samra, A. B., Freeman, M., Kong, X. F., Schipani, E., Richards, J., Kolakowski, L. F., Jr., Hock, J., Potts, J. T., Jr., and Kronenberg, H. M., et al. (1991) *Science 254*, 1024−1026.

9. Pines, M., Fukayama, S., Costas, K., Meurer, E., Goldsmith, P. K., Xu, X., Muallem, S., Behar, V., Chorev, M., Rosenblatt, M., Tashjian, A. H., Jr., and Suva, L. J. (1996) *Bone 18*, 381−389.
10. Suva, L. J., Mather, K. A., Gillespie, M. T., Webb, G. C., Ng, K. W., Winslow, G. A., Wood, W. I., Martin, T. J., and Hudson, P. J. (1989) *Gene 77*, 95−105.
11. Potts, J. T., Jr., Tregear, G. W., Keutmann, H. T., Niall, H. D., Sauer, R., Deftos, L. J., Dawson, B. F., Hogan, M. L., and Aurbach, G. D. (1971) *Proc. Natl. Acad. Sci. U.S.A. 68*, 63−67.
12. Kemp, B. E., Moseley, J. M., Rodda, C. P., Ebeling, P. R., Wettenhall, R. E., Stapleton, D., Diefenbach-Jagger, H., Ure, F., Michelangeli, V. P., Simmons, H. A., and et al. (1987) *Science 238*, 1568−1570.
13. Nissenson, R. A., Diep, D., and Strewler, G. J. (1988) *J. Biol. Chem. 263*, 12866−12871.
14. Nussbaum, S. R., Rosenblatt, M., and Potts, J. T., Jr. (1980) *J. Biol. Chem. 255*, 10183−10187.
15. Juppner, H., Abou-Samra, A. B., Uneno, S., Gu, W. X., Potts, J. T., Jr., and Segre, G. V. (1988) *J. Biol. Chem. 263*, 8557−8560.
16. Usdin, T. B., Gruber, C., and Bonner, T. I. (1995) *J. Biol. Chem. 270*, 15455−15458.
17. Gardella, T. J., Luck, M. D., Jensen, G. S., Usdin, T. B., and Jüppner, H. (1996) *J. Biol. Chem. 271*, 19888−19893.
18. Behar, V., Pines, M., Nakamoto, C., Greenberg, Z., Bisello, A., Stueckle, S. M., Bessalle, R., Usdin, T. B., Chorev, M., Rosenblatt, M., and Suva, L. J. (1996) *Endocrinology 137*, 2748−2757.
19. Behar, V., Nakamoto, C., Greenberg, Z., Bisello, A., Suva, L. J., Rosenblatt, M., and Chorev, M. (1996) *Endocrinology 137*, 4217−4224.
20. Draper, M. W., Nissenson, R. A., Winer, J., Ramachandran, J., and Arnaud, C. D. (1982) *J. Biol. Chem. 257*, 3714−3718.
21. Zhou, A. T., Bessalle, R., Bisello, A., Nakamoto, C., Rosenblatt, M., Suva, L. J., and Chorev, M. (1997) *Proc. Natl. Acad. Sci. U.S.A. 94*, 3644−3649.
22. Bisello, A., Adams, A. E., Mierke, D. F., Pellegrini, M., Rosenblatt, M., Suva, L. J., and Chorev, M. (1998) *J. Biol. Chem. 273*, 22498−22505.
23. Mannstadt, M., Luck, M. D., Gardella, T. J., and Juppner, H. (1998) *J. Biol. Chem. 273*, 16890−16896.
24. van Buuren, A. R., Marrink, S., and Berendsen, H. J. C. (1993) *J. Phys. Chem. 97*, 9206−9216.
25. Vriend, G. (1990) *J. Mol. Graph. 8*, 52−56.
26. Henderson, R., Baldwin, J. M., Ceska, T. A., Zemlin, F., Beckmann, E., and Downing, K. H. (1990) *J. Mol. Biol. 213*, 899−929.
27. Schertler, G. F., Villa, C., and Henderson, R. (1993) *Nature 362*, 770−772.
28. Schertler, G. F., and Hargrave, P. A. (1995) *Proc. Natl. Acad. Sci. U.S.A. 92*, 11578−11582.
29. Grigorieff, N., Ceska, T., Downing, K., Baldwin, J., and Henderson, R. (1996) *J. Mol. Biol. 259*, 393−421.
30. Pellegrini, M., Bisello, A., Rosenblatt, M., Chorev, M., and Mierke, D. F. (1998) *Biochemistry 37*, 12737−12743.
31. Paterlini, G., Portoghese, P. S., and Ferguson, D. M. (1997) *J. Med. Chem. 40*, 3254−3262.
32. Altschul, S. F., Madden, T. L., Schaffer, A. A., Zhang, J., Zhang, Z., Miller, W., and Lipman, D. J. (1997) *Nucleic Acids Res. 25*, 3389−3402.
33. Bernstein, F. C., Koetzle, T. F., Williams, G. J. B., Meyer, E., Bryce, M. D., Rogers, J. R., Kennard, O., Shikanouchi, T., and Tasumi, M. (1977) *J. Mol. Biol. 112*, 535.
34. Berendsen, H. J. C., van der Spoel, D., and van Buuren, R. (1995) *Comput. Phys. Commun. 95*, 43−56.
35. Pellegrini, M., Royo, M., Rosenblatt, M., Chorev, M., and Mierke, D. F. (1998) *J. Biol. Chem. 273*, 10420−10427.
36. Bundi, A., Andreatta, R., Rittel, W., and Wuthrich, K. (1976) *FEBS Lett. 64*, 126−129.
37. Klaus, W., Dieckmann, T., Wray, V., Schomburg, D., Wingender, E., and Mayer, H. (1991) *Biochemistry 30*, 6936−6942.
38. Neugebauer, W., Surewicz, W. K., Gordon, H. L., Somorjai, R. L., Sung, W., and Willick, G. E. (1992) *Biochemistry 31*, 2056−2063.
39. Barden, J. A., and Cuthbertson, R. M. (1993) *Eur. J. Biochem. 215*, 315−321.
40. Wray, V., Federau, T., Gronwald, W., Mayer, H., Schomburg, D., Tegge, W., and Wingender, E. (1994) *Biochemistry 33*, 1684−1693.
41. Neugebauer, W., Barbier, J.-R., Sung, W. L., Whitfield, J. F., and Willick, G. E. (1995) *Biochemistry 34*, 8835−8842.
42. Berendsen, H. J. C., Postma, J. P. M., DiNola, A., and Haak, J. R. (1984) *J. Chem. Phys. 81*, 3684−3690.
43. Baldwin, J. M. (1993) *EMBO J. 12*, 1693−1703.
44. Czaplewski, C., Kazmierkiewicz, R., and Ciarkowski, J. (1998) *J. Comput. Aided Mol. Des. 12*, 275−287.
45. Beck, M., Sakmar, T. P., and Siebert, F. (1998) *Biochemistry 37*, 7630−7639.
46. Bourne, H. R. (1997) *Curr. Opin. Cell Biol. 9*, 134−142.
47. Gardella, T. J., Luck, M. D., Fan, M. H., and Lee, C. (1996) *J. Biol. Chem. 271*, 12820−12825.
48. Schipani, E., Langman, C. B., Parfitt, A. M., Jensen, G. S., Kikuchi, S., Kooh, S. W., Cole, W. G., and Jüppner, H. (1996) *New Engl. J. Med. 335*, 708−714.
49. Schipani, E., Jensen, G. S., Pincus, J., Nissenson, R. A., Gardella, T. J., and Juppner, H. (1997) *Mol. Endocrinol. 11*, 851−858.
50. Schipani, E., Hunzelman, J., Langman, C. B., and Juppner, H. (1998) *American Society for Bone and Mineral Research*, pp 254, Elsevier, San Francisco.
51. Lee, C., Luck, M. D., Juppner, H., Potts, J. T. Jr., Kronenberg, H. M., and Gardella, T. J. (1995) *Mol. Endocrinol. 9*, 1269−1278.
52. Winnik, M. A. (1981) *Chem. Rev. 81*, 491−534.
53. Clark, J. A., Bonner, T. I., Kim, A. S., and Usdin, T. B. (1998) *Mol. Endocrinol. 12*, 193−206.
54. Mierke, D., and Pellegrini, M. (1999) *Curr. Pharm. Des. 5*, 21−36.
55. Gardella, T. J., Luck, M. D., Wilson, A. K., Keutmann, H. T., Nussbaum, S. R., Potts, J. T., Jr., and Kronenberg, H. M. (1995) *J. Biol. Chem. 270*, 6584−6588.
56. Bergwitz, C., Jusseaume, S. A., Luck, M. D., Juppner, H., and Gardella, T. J. (1997) *J. Biol. Chem. 272*, 28861−28868.
57. Turner, P. R., Mefford, S., Bambino, T., and Nissenson, R. A. (1998) *J. Biol. Chem. 273*, 3830−3837.
58. Frelinger, I., A. L., and Zull, J. E. (1984) *J. Biol. Chem. 259*, 5507−5513.
59. Rosenblatt, M., Goltzman, D., Keutmann, H. T., Tregear, G. W., and Potts, J. T., Jr. (1976) *J. Biol. Chem. 251*, 159−164.
60. Cohen, F. E., Strewler, G. J., Bradley, M. S., Carlquist, M., Nilsson, M., Ericsson, M., Ciardelli, T. L., and Nissenson, R. A. (1991) *J. Biol. Chem. 266*, 1997−2004.
61. Greiner, G., Dornberger, U., Paegelow, I., Scholkens, B. A., Liebmann, C., and Reissmann, S. (1998) *J. Pept. Sci. 4*, 92−100.
62. Ciucci, A., Palma, C., Manzini, S., and Werge, T. M. (1998) *Br. J. Pharmacol. 125*, 393−401.
63. Pesek, M. J., Howe, N., and Sheridan, M. A. (1998) *Gen. Comp. Endocrinol. 112*, 183−90.
64. Li, H., Leeman, S. E., Slack, B. E., Hauser, G., Saltsman, W. S., Krause, J. E., Blusztajn, J. K., and Boyd, N. D. (1997) *Proc. Natl. Acad. Sci. U.S.A. 94*, 9475−9480.
65. Sargent, D. F., and Schwyzer, R. (1986) *Proc. Natl. Acad. Sci. U.S.A. 83*, 5774−5778.
66. Schwyzer, R. (1991) *Biopolymers 31*, 785−792.
67. Schwyzer, R. (1992) *Braz. J. Med. Biol. Res. 25*, 1077−1089.
68. Moroder, L., Romano, R., Guba, W., Mierke, D. F., Kessler, H., Delporte, C., Winand, J., and Christophe, J. (1993) *Biochemistry 32*, 13551−13559.
69. Elling, C. E., Nielsen, S. M., and Schwartz, T. W. (1995) *Nature 374*, 74−77.
70. Elling, C. E., and Schwartz, T. W. (1996) *EMBO J. 15*, 6213−6219.

BI9829276